NON-OPTICAL SURFACE TOPOGRAPHY BY PROJECTED INTERFERENCE FRINGES

O. D. D. SOARES

Centro de Física, Universidade do Porto
4000 Porto, Portugal

ABSTRACT — Optical measurement techniques have always played an important role in precision metrology. Surface topography is a topic of great interest to science, technology and industry. Application of the technique of projected interference fringes in non-optical surface topography is described. Details and limitations of the technique are discussed. Prospects associated with the introduction of digital image processing are outlined.

1 — INTRODUCTION

In recent years several papers have been published on methods using projected fringes for various measurements on three-dimensional objects [1]-[9].

The projected fringes methods were mostly applied to problems of contouring, deformation measurement and vibration analysis. It has also been reported the application in dimensional metrology, surface inspection of parts used in mechanical engineering, and image recognition of surface defects.

In our case we were dealing with measurement of flatness of a plane surface of piston rings. The method was further tested on a dimensionally controlled cylindrical surface machined on

Portgal. Phys. — Vol. 13, fasc. 3-4, pp. 217-231, 1982

217

brass. The later results led to a more detailed examination of the method; its limitations were then established and the need for computer image processing emerged.

2 — PRINCIPLE OF THE METHOD

Fringe illumination is a spatially coded illumination of the object to obtain three-dimensional information.

Rowe and Welford [1] presented a method for the study of surface topography by projecting obliquely on a surface a set of interference fringes produced by two collimated coherent beams intersecting at an angle. The interference fringes are formed in the overlapping volume of the beams as planes parallel to the bisector of the angle, 2ϕ, between the beams. The intersection of these fringes' planes with the surface represents codified information of the surface topography.

The spatial invariance of the interference fringes means that there is no limit on the depth for application of the method, within the interfering volume of the two beams.

The fringe spacing, in principle, can have any value between $\lambda/2$ (λ being the radiation wavelength), and the major transversal dimension of the object area simultaneously illuminated by the two beams [10]. In pratice the method is applied with fringe spatial periods over a range from 1 μm to several millimeters so that the precision is variable over this range [2]. The papers quoted [1]-[9] describe methods of producing the fringes, optimum condition of use, extensions of the method and various applications. A detailed study of the method is presented in the following sections.

3 — FRINGE PATTERN CHARACTERISTICS AND METHOD LIMITATIONS

The important features of the fringe pattern are:

i) Fringe visibility or contrast.

ii) Fringe spatial frequency spectrum.

iii) Fringe spatial orientation.

iv) Fringe to surface topography correlation.

Fringe visibility is well studied in the scientific literature [11] in relation to its dependence on the degree of coherence between the interfering beams, the angle between the directions of polarization of the beams, and the intensity ratio of the beams. In some cases surface reflectivity can also be adjusted to enhance fringe contrast. Optimized fringe visibility should be attempted to facilitate experimental implementation and relax limitations on the viewing and recording system of the projected fringes.

The fringe frequency v for the two plane waves with normalized wave-vectors; $\mathbf{u}_1$ (u_{1x}, u_{1y}, u_{1z}) and $\mathbf{u}_2$ (u_{2x}, u_{2y}, u_{2z}), is given by [12]

$$v = (1/\lambda) \{ |2(1 - u_{1x}\, u_{2x} - u_{1y}\, u_{2y}) - (u_{1z}^2 + u_{2z}^2)| \}^{1/2} \qquad (1)$$

where λ is the radiation wavelength, and the z-axis was chosen normal to the surface of observation. In order to simplify the interpretation of the experimental results an incidence within a plane normal to the studied surface is assumed so that v comes

$$v = |(\sin \phi_1 + \sin \phi_2)/\lambda| = 1/d \qquad (2)$$

where ϕ_1 and ϕ_2 are the angles between the beams and the normal to the surface of observation.

An equivalent formula in terms of 2ϕ, the angle between the beams, and β, the angle between the normal to the surface and the bisector of angle 2ϕ, is

$$v = 2|\sin \phi\, \cos \beta / \lambda| = 1/d \qquad (3)$$

where d is again the fringe spatial period.

Experiments are performed under the assumption that it is valid to adopt expression (3), considering the angles defined through the local average normal to the surface under study and v representing the local average frequency of the fringes seen on the surface.

The spatial orientation of the fringes results from the geometry of interception of the surface under examination by

the fringe system. The fringe system is a family of parallel planes, within the interference field, equally spaced and normal to a plane parallel to the directions of the interfering beams. In a cartesian coordinate system, with the y-direction parallel to the fringe system, the object surface can be written

$$z = f(x, y) \tag{4}$$

The set of equally spaced fringe planes is given by the equation

$$z' = (x - nd) / tg\,\beta \tag{5}$$

where $n = 0, 1, 2, 3...$, d is the spacing (in the x direction) of the planes, and β the angle of the planes with the z axis. The fringes on the surface are given by

$$x = f(x, y)\,tg\,\beta + nd \tag{6}$$

The analysis simplifies if the surface is assumed flat and the plane parallel to the directions of the interfering beams is normal to the surface. Thus, the fringes to surface topography correlation can be established in localized areas. If a step of height h exists, the fringe system will show a displacement

$$\Delta = h\,|tg\,\beta| \tag{7}$$

when viewed along the surface normal, Fig. 1. For $\beta = 0$ an oblique observation of the fringes on the surface must be done. This will be discussed further on. The fringe distance variation, Δ, in practice, could correspond to either a fringe interspace contraction or enlargement. This is certainly explained by the two possibilities of a down and up step surface accident. The distinction is not so simple to establish because it is relative to the direction in which the surface is explored and to the fringe illumination incidence. A possible way of giving a correct interpretation is to assume that an observer travels with the plane normal to the fringe system towards the surface under examination. If an enlargement is observed a down step has been localized. Alternatively, the fringe contraction would reveal an up step on the surface.

220

Portgal. Phys. — Vol. 13, fasc. 3-4, pp. 217-231, 1982
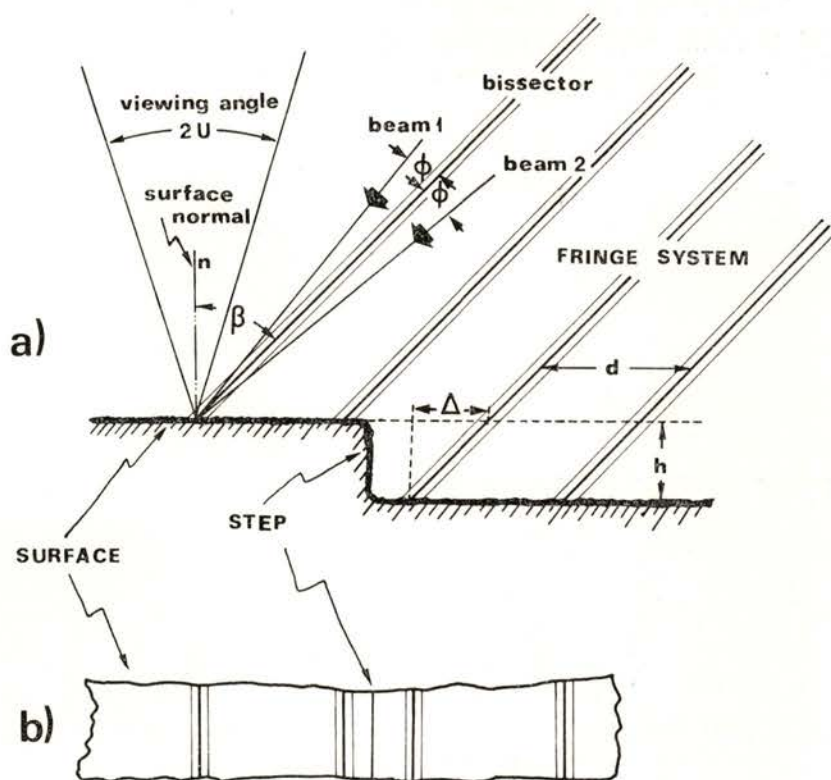
Fig. 1 — Displacement $\Delta = h\,|\,tg\,\beta\,|$ of the fringes on the surface due to a step of height h ; observation normal to the surface : *a*) Lateral view ; *b*) Top view.

The displacement Δ compares to the fringe period as

$$|\,\Delta\,/\,d\,| \;=\; 2\,|\,h\,\sin\phi\,\sin\beta\,/\,\lambda\,| \tag{8}$$

If observation is made at an angle γ (relative to the normal to the surface) the value of the recorded d_γ is then (Fig. 2)

$$d_\gamma = d\,\cos\gamma \tag{9}$$

and the fringe displacement Δ_γ comes as

$$\Delta_\gamma = h\,|\,\sin(\beta\text{-}\gamma)\,|\,/\,\cos\beta \tag{10}$$

It is seen that condition $\beta \neq \gamma$ should be satisfied.

The method limitations [2] in practice are imposed by the optical viewing system (microscope). The smallest fringe spacing that can be resolved by the optical system with a numerical
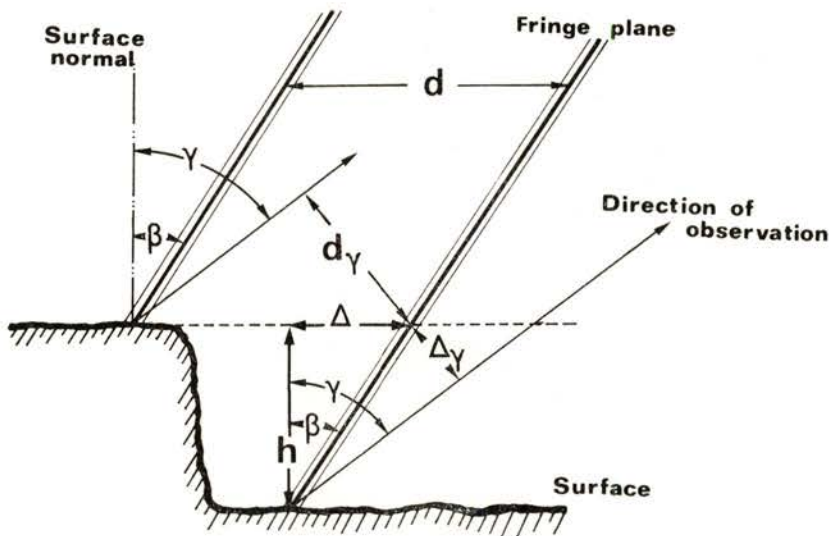
Fig. 2 — Displacement Δ_γ of the fringes on the surface due to a step of height h when observed at an angle γ.

aperture equal to sin U is 0.5 λ/sin U ; the corresponding focal depth is $\pm \lambda / (8 \sin^2 U/2)$.

To resolve the fringes one should have

$$\sin U > \sin \phi \, \cos \beta \tag{11}$$

To see the fringes across a step of height h without refocusing one must have

$$\sin^2 (U/2) < \lambda / 8h \tag{12}$$

Therefore the fringes would have the lowest spatial frequency for the required purpose in order to resolve them, while ensuring fringe structure in focus throughout full depth (this also attenuates problems of vibration stability). A compromise should be sought between the two conflicting requirements, depth of field and

lateral resolution. If a depth of field $\pm h$ is desired then the smallest distance resolvable laterally is

$$[\,(\lambda h/2\,)\,/\,(\,1 - \lambda/8h\,)\,]^{1/2} \qquad (13)$$

or, to an approximation acceptable for many purposes, $(\lambda h/2\,)^{1/2}$. This applies for an observing system not refocusable.

Fringe spacing has, in theory, no upper limit; but a lower limit is imposed by practical reasons as seen from Fig. 1, corresponding to $2\phi = \beta = 2\,U = 45°$. For $\lambda = 0.6328\ \mu m$ this gives for fringe spacing a value of $1.17\ \mu m$.

It should be noticed that the examinable area depends on the coherence of the source. For narrow fringe spacing the area has to be observed through a microscope so that coherence is not a major constraint in practice. However, the effect of speckle may impose cutting down the numerical aperture of the viewing system [2] with a spatial frequency cutoff beyond the projected fringes frequency and below the higher spatial frequencies corresponding to the speckle. The use of large fringes for the examination of large areas may be limited by the coherence of the source and could impose the use of a direct moiré technique.

The method relies on the assumption that the fringe system is a set of equidistant parallel planes. The interfering beams must then present a plane phase wavefront. In practice one should expect departures from the ideal conditions so that tolerance ranges have to be examined. In fact, a remanent angular divergence of the beam α could still be accounted for. From expression (2) it can be seen that the fringe spacing on the surface is perturbed within a range of

$$d\,(\,1 \pm \alpha\,/\sin\phi\,) \qquad (14)$$

For simplicity of the analysis it was assumed $\gamma \neq \beta = 0$.
The divergence, α, should then be much smaller than

$$2\,(\,h\,/\lambda\,)\ \mathrm{tg}\,\phi\ \sin\phi\ \mathrm{tg}\,\gamma \qquad (15)$$

a not very stringent condition in practice. A more general solution leads to the conclusion

$$|\,1\,/\sin\,(\,\phi + \alpha\,) - 1/\sin\phi\,| \ll (\,h/2\,\lambda\,)\,|\sin\,(\,\beta - \gamma\,)\,| \qquad (16)$$

The divergence of the beams results, in practice, in a variation of the spatial frequency across the field; however, if proper care is taken, the method could still be applied.
The divergence has to be small, otherwise the fringe system will form on a curved family of surfaces adding, in general, unnecessary complexity to the problem.

From eq (10) one can easily establish the relation between the absolute errors (ε) of the quantities h, β, γ, Δ_γ:

$$\varepsilon(h)/h = \varepsilon(\Delta_\gamma)/\Delta_\gamma + \varepsilon(\gamma)|tg(\beta\text{-}\gamma)|^{-1} + \varepsilon(\beta)(tg\,\beta + |tg(\beta\text{-}\gamma)|^{-1})$$

(17)

The relative error on the measurement of h is of the same order as that obtained on the recording of Δ_γ assuming that β and γ are adequately measured (what does not present practical difficulties).
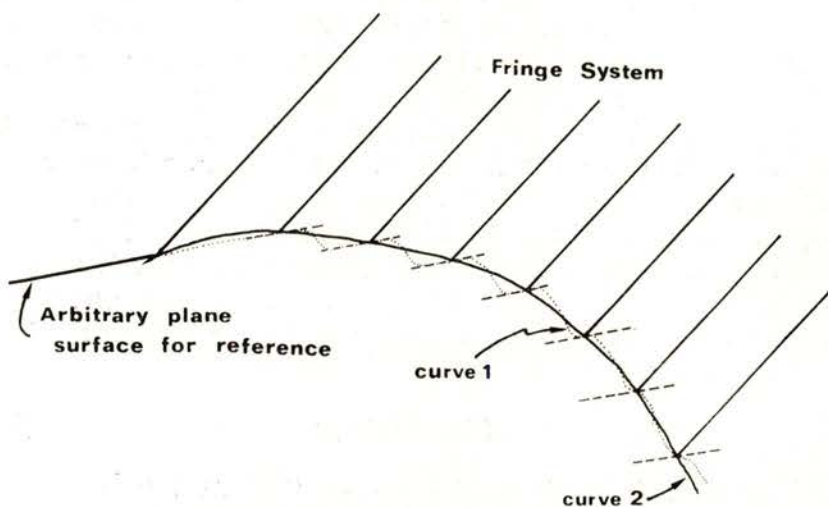
Fig. 3 — Fringe system interpretation with surface profile uncertainty resulting from a step by step method: curve 1 — step by step reading of the surface; curve 2 — real curved surface.

Another problem to be discussed relates to the process of observation of the fringes on the surface. Whether viewed directly

or photographed the fringes system suffers an anamorphic distortion which must be corrected. The photographic system, taken as example, is equivalent to a central point transformation of the points of the object photographed into the points of the plane of the photographic film. According to Fig. 2 and expression (10) the step of height h leads to a fringe spacing deviation on the photographic film Δ_γ which varies over $\delta_\gamma = U$ (Fig. 1), i.e. the range of permitted variation of the angle of observation. Care should then be taken in examining the implications of the recording geometry. Once β has been chosen to be large, γ very small and δ_γ small, this effect is negligible in most of the cases that were here considered. Alternatively a telecentric viewing system can be used. Nevertheless, for the general case, as the effect varies over the field of view it has to be compensated. This can easily be done through computer image processing techniques.

Finally, the spatial iterative character of the method leads to a step by step approximation — curve 1 of Fig. 3, of a curved surface under examination — curve 2. Therefore the localization of the step is undefined within the fringe interspacing. Such a limitation suggests the analysis of the surface by moving the fringes system over the surface (e.g. using phase modulation of one of the beams) and a computer based analysis. This constitutes one of the motivations for this work, namely the introduction of image processing techniques.

4 — EXPERIMENTAL RESULTS

The fringe system can be obtained by several methods described in detail in the literature [1], [2], [5]-[7].

The experimental arrangement we used is shown in Fig. 4. Two collimated beams intercept at a large angle (typical values, $\phi = 3°$, $\beta = 45°$) using a conventional expander, collimator, beam splitter and front surface mirror. Other types of interferometers could also be used, in particular those producing shearing of the interfering beams.

The surface under examination is placed within the beams interference volume and a microscope, with a photographic camera
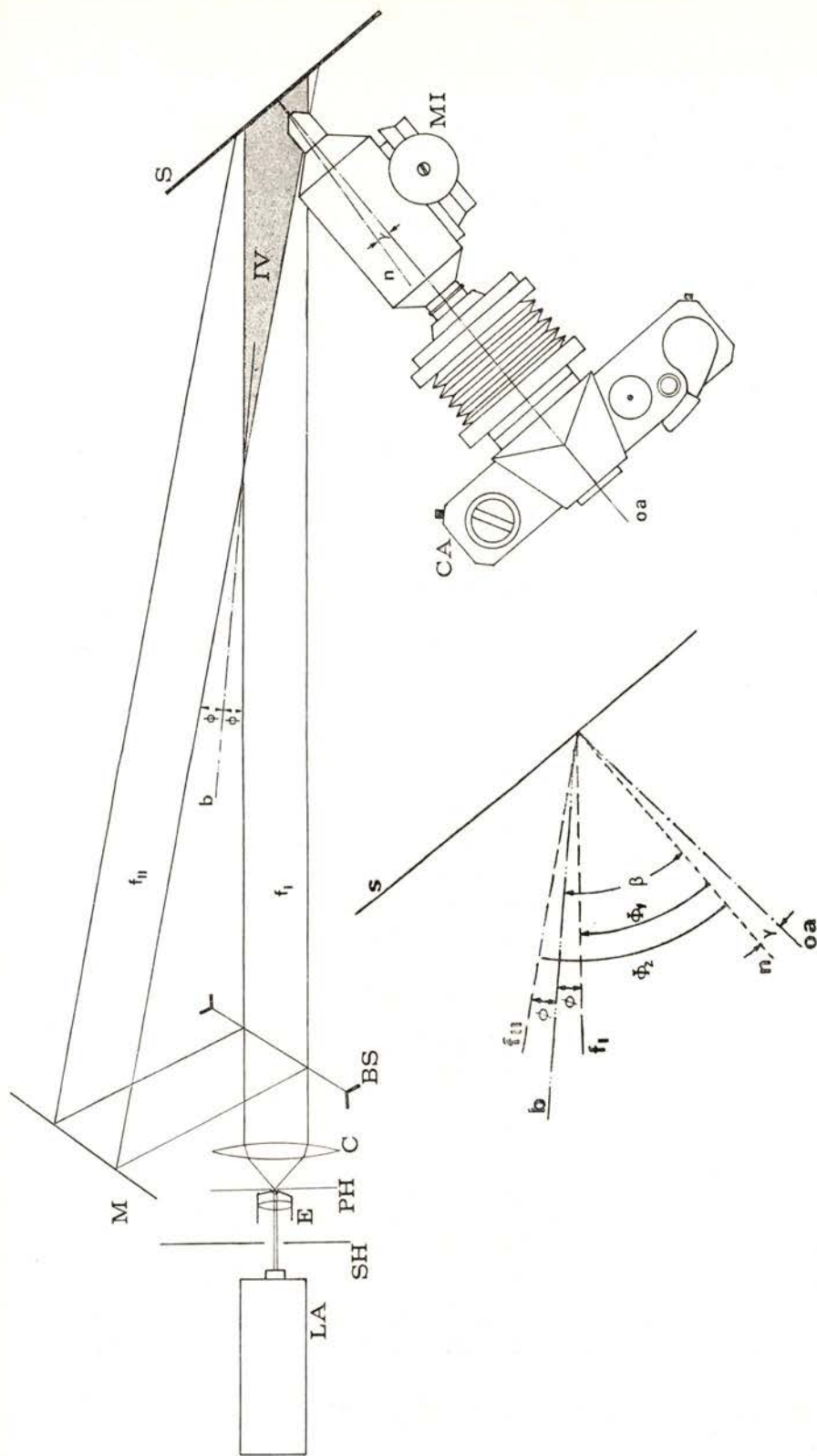
Fig. 4 — Schematic representation of the experimental arrangement: LA—laser; SH—shutter; E—expander; PH—pinhole; C—collimating lens; BS—beam splitter; M—mirror; MI—microscope; CA—photographic camera; S—surface under examination. The figure recalls also the definition of geometrical parameters.

attached, is used for viewing and recording the fringes over the surface (typical value $\gamma = 1°$).

The fringe spacing was adjusted in a range $5 \ \mu m - 16 \ \mu m$. Figure 5 shows the projected fringes on the flat surface of a piston ring under study. The fringe planes distance was $8.1 \ \mu m$ ($\phi = 2.2°$) and the spatial period over the plane surface $11.5 \ \mu m$ ($\beta = 45°$); the photograph was taken along the normal to the surface ($\gamma = 0$). This image was explored using a graphic scale, Fig. 6, because the moiré technique showed very large fringes. The scale is made of parallel lines dimensionally equivalent to the fringe system over the surface and a set of small thicker traces. The edges of these traces were drawn to represent successive fringe spacing variations by one tenth of the fringe spacing. In the case illustrated a variation 'down' $h = 6.9 \ \mu m$ on the surface relief was found. Certainly much more information is contained in Fig. 5, but it is most advisable to proceed by using a computer technique, the ultimate aim of our project; then a computed surface profile could be drawn.

5 — APPLICATIONS OF THE METHOD

The method finds application in dimensional metrology, mainly surface topography, vibration analysis [13] and contouring through combination with other techniques like moiré (in the comparison of surfaces). Changes in surface configuration either by distortion, deformation or substitution can be measured [14].

Non-destructive testing (micro-mechanics, crack and flaw detection, etc.) and the application, in a transmission arrangement, to phase objects is also considered relevant. Further, holographic recording of the fringe system on the surface and later analysis with real image projection may be of some value for some applications.

6 — CONCLUSION

A simple interference fringe projection technique has been described. It is quantitative, non-contact, requires no surface
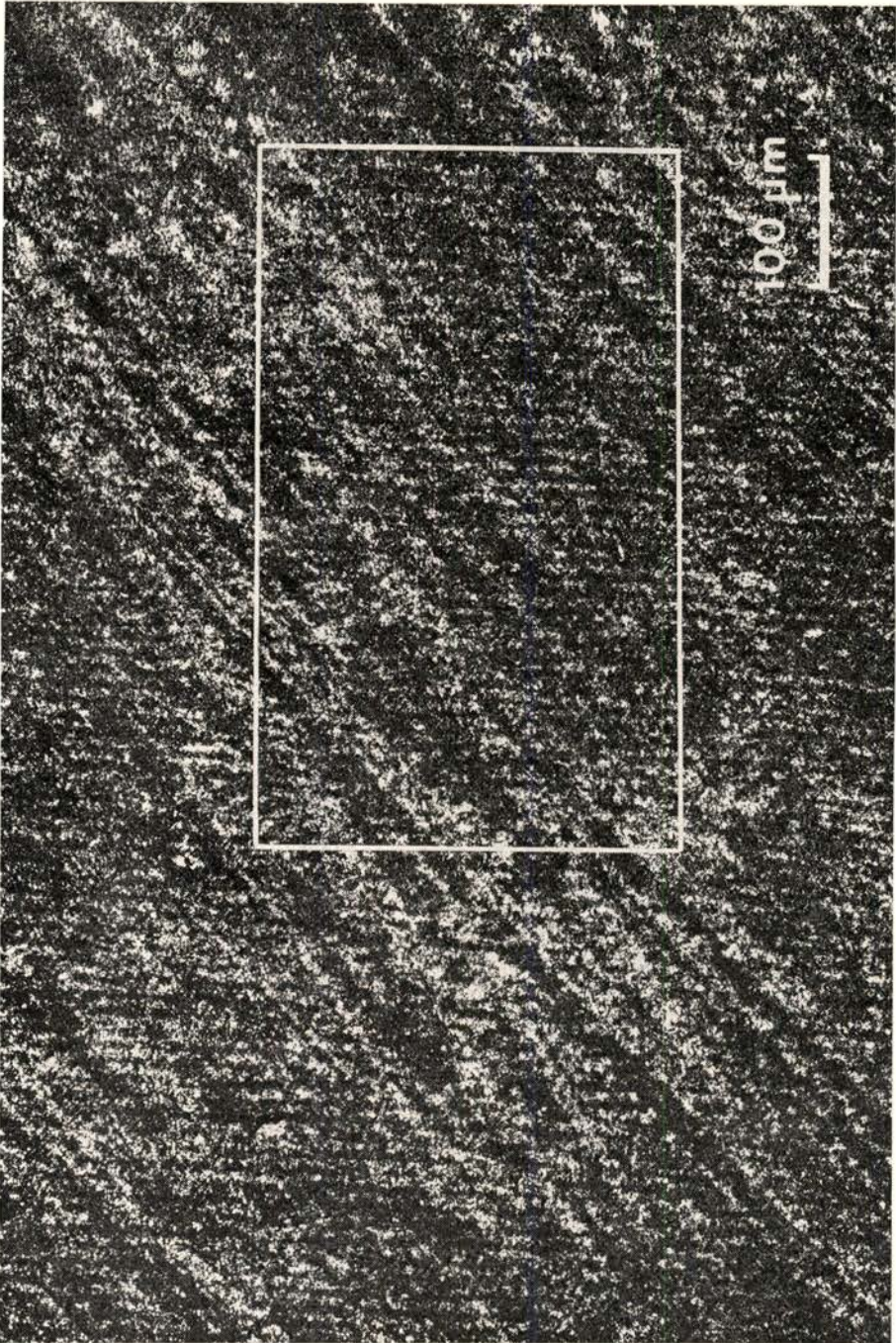
Fig. 5a — Projected fringes on a surface: general aspect of the microscopic field of view.
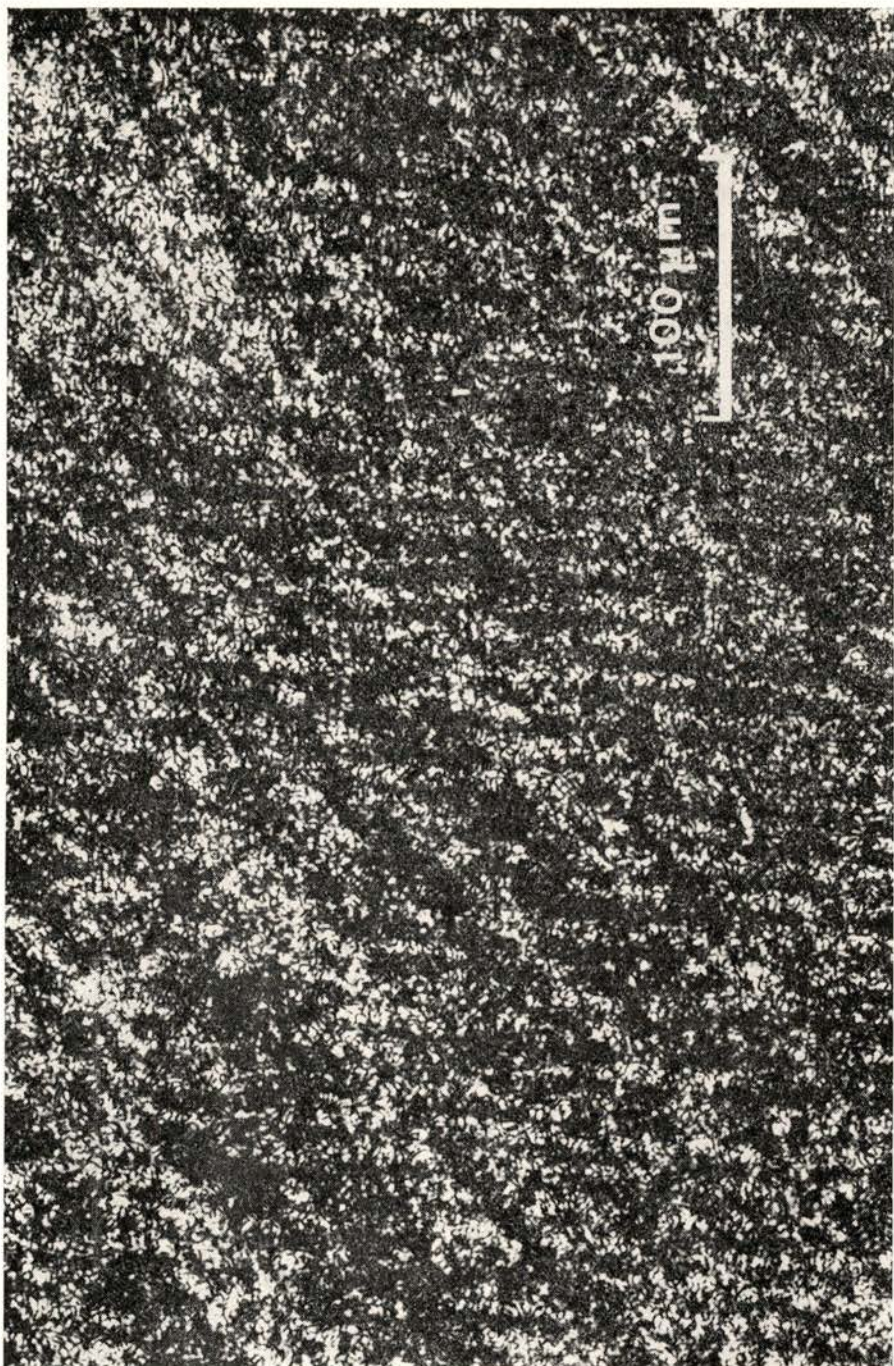
Fig. 5b — Projected fringes on a surface : enlarged detail corresponding to area marked in 5a.

preparation, is adequate for real time studies and for automatization, having a measurement sensitivity adjustable within a broad range. The fringe pattern has a simple quantitative de-
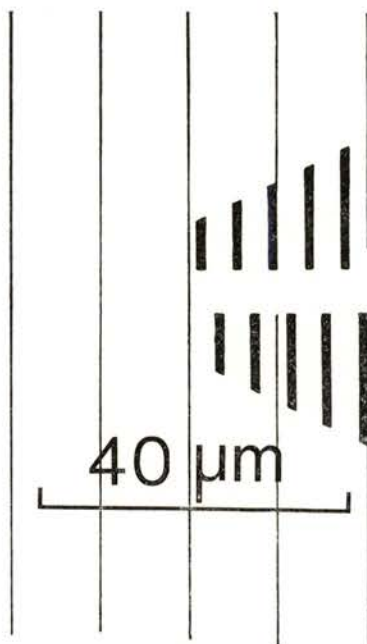
Fig. 6 — Graphic scale expressed on fringe interspacing tenths.

scription and interpretation. A detailed study of the method and its implementation revealed that result analysis must proceed by recourse to computer image processing techniques.

Much of the experimental work and drawings were skillfully performed by J. A. Fernandes in cooperation with J. S. Fernandes.

REFERENCES

[1]   S. H. Rowe, W. T. Welford, *Nature,* **216** (1967), 786.

[2]   W. T. Welford, *Optica Acta* **16** (1969), 371.

[3]   S. H. Rowe, *J. Opt. Soc. Am.* **61** (1971), 1599.

[4]   A. J. MacGovern, *Appl. Opt.* **11** (1972), 2972.

[5]   C. G. Murphy, *ISA ASIT,* 74201 (1974), 1.

[6]   P. Benoit, *Thèse,* Univ. Paris-Sud (1974).

[7]   P. Benoit, E. Mathieu, J. Hormière, A. Thomas, *Nouv. Rev. Optique* **6** (1975). 67.

[8]   B. Dessus, J. P. Gerardin, P. Mousselet, *Optical and Quantum Electr.* **7** (1975), 15.

[9]   G. Indebetouw, *Appl. Opt.* **17** (1978), 2930.

[10] O. D. D. Soares, *Appl. Opt.* **18** (1978), 3838.

[11] K. Leonhardt, *Optik* **41** (1974), 344.

[12] O. D. D. Soares, *Thesis,* U. London (1976).

[13] P. Spicer, B. M. Watrasiewicz, *Optica Acta* **15** (1968), 521.

[14] R. E. Brooks, L. O. Heflinger, *Appl. Opt.* **8** (1969), 935.